

**Coupled Modeling of Non-isothermal Multi-phase Flow, Solute
Transport and Reactive Chemistry in Porous and Fractured Media:
1. Model Development and Validation**

Tianfu Xu and Karsten Pruess

Earth Sciences Division, Lawrence Berkeley National Laboratory, University of California,
Berkeley, CA 94720.

Submitted to *Journal of Geophysical Research*

September 1998

This work was supported by the Laboratory Directed Research and Development Program of the Ernest Orlando Lawrence Berkeley National Laboratory under Contract No. DE-AC03-76SF00098 with the U.S. Department of Energy.

Coupled modeling of non-isothermal multiphase flow, solute transport and reactive chemistry in porous and fractured media:

1. Model development and validation

Tianfu Xu and Karsten Pruess

Earth Sciences Division, Lawrence Berkeley National Laboratory, University of California, Berkeley, CA 94720

Abstract. Coupled modeling of subsurface multiphase fluid and heat flow, solute transport and chemical reactions can be used for the assessment of acid mine drainage remediation, mineral deposition, waste disposal sites, hydrothermal convection, contaminant transport, and groundwater quality. Here we present a numerical simulation model, TOUGHREACT, which considers non-isothermal multi-component chemical transport in both liquid and gas phases. A wide range of subsurface thermo-physical-chemical processes is considered. The model can be applied to one-, two- or three-dimensional porous and fractured media with physical and chemical heterogeneity. The model can accommodate any number of chemical species present in liquid, gas and solid phases. A variety of equilibrium chemical reactions is considered, such as aqueous complexation, gas dissolution/exsolution, cation exchange, and surface complexation. Mineral dissolution/precipitation can proceed either subject to local equilibrium or kinetic conditions. The coupled model employs a sequential iteration approach with reasonable computing efficiency. The development of the governing equations and numerical

approach is presented along with the discussion of the model implementation and capabilities. The model is verified for a wide range of subsurface physical and chemical processes. The model is well suited for flow and reactive transport in variably saturated porous and fractured media. In the second of this two-part paper [this issue], three applications covering a variety of problems are presented to illustrate the capabilities of the model.

1. Introduction

Coupled modeling of subsurface multiphase fluid and heat flow, solute transport and chemical reactions can be used for the assessment of mineral deposits, acid mine drainage remediation, waste disposal sites, the analysis of hydrothermal convection systems, the study of contaminant transport, and the understanding of groundwater quality. In the past decade, a number of models accounting for subsurface physical and chemical processes have been developed. Two major approaches have been used to couple multi-species transport and chemistry: (1) direct substitution approach (DSA), which substitutes the chemical reaction equations directly into the transport equations; and (2) sequential iteration approach (SIA), which solves the transport and the reaction equations separately in a sequential manner with an iterative procedure. The use of the DSA leads to a system of fully coupled highly nonlinear transport equations. Its advantage is high accuracy, but its main disadvantage is a very high demand on computing resources [Yeh and Tripathi, 1989]. Because of the computational demands it may be impractical to apply this approach to field scale 2- and 3-D problems. In the SIA, since the sets of equations that are solved

simultaneously are much smaller than in the DSA, larger systems with larger sets of chemical species can be handled. The SIA method has been widely used by many investigators, such as *Cederberg et al.* [1985], *Ague and Brimhall* [1989], *Liu and Narasimhan* [1989], *Engesgaard and Kipp* [1992], *Nienhuis et al.* [1991], *Yeh and Tripathi* [1991], *Simunek and Soares* [1994]; *Walter et al.* [1994], *Zysset et al.* [1994], *Lichtner* [1996], *Steeffel and MacQuarrie*. [1996], *Viswanathan* [1996], *Neretnieks et al.* [1997], *Sun et al* [1998], and *Xu et al.* [1998a].

An important aspect of any reactive transport model is its ability to deal with a wide range of subsurface thermo-physical-chemical processes in field scale complex geologic media. Most often, available models consider only isothermal conditions ignoring temperature effects even though chemical processes depend strongly on temperature. Only a few models incorporate heat transport. Most models are suitable only for simulating reactive transport in saturated porous media, and limit the flow and transport to the liquid phase. Here we present a general coupled model, TOUGHREACT, which considers non-isothermal multi-component chemical transport in both liquid and gas phases. A wide range of subsurface thermo-physical-chemical processes is considered. The model can be applied to one-, two-, or three-dimensional porous and fractured media with physical and chemical heterogeneity. For flow and transport in fractured media, a double porosity and dual permeability model is included. The model can accommodate any number of chemical species present in liquid, gas and solid phases. Chemical reactions considered under the local equilibrium assumption are aqueous complexation, acid-base, redox, gas dissolution/exsolution, cation exchange, and surface complexation. Mineral dissolution/precipitation can proceed either subject to local equilibrium or kinetic

conditions. Reaction effects on porosity, permeability, density and viscosity are neglected. The coupled model employs a sequential iteration approach that is viewed as the most straightforward technique for achieving a comprehensive modeling capability with reasonable computing efficiency. This approach allows applications to field scale reactive chemical transport problems where a large number of equations are required to be solved. The computer simulator was developed by introducing solute transport and reactive chemistry into the framework of the existing non-isothermal multiphase flow simulator TOUGH2 [Pruess, 1991]. The model has been verified for a variety of physical and chemical processes. A simulation of water quality in the Aquia aquifer (Maryland) is performed to validate the model for field scale problems.

We first present the development of governing equations for non-isothermal multiphase flow, solute transport and chemical reactions. Then the numerical implementation and model capabilities are addressed. Finally the verification and validation are presented. In the second of this two-part paper [this issue], three applications covering a variety of reactive transport problems are presented to illustrate the model capabilities, including (1) supergene copper enrichment in unsaturated-saturated media; (2) thermo-hydro-chemical modeling for the drift scale heater test at Yucca Mountain, Nevada; and (3) chemical evolution in irrigated soil.

2. Model formulation

2.1. Non-isothermal multiphase flow and multi-component transport

In the present work, major assumptions are made as follows: (1) porosity and permeability change from mineral dissolution/precipitation is neglected, (2) aqueous chemical concentration changes do not influence fluid thermophysical properties such as density and viscosity, (3) changes in partial pressure of gases other than H₂O and air (i.e. trace gases such as CO₂ and O₂) due to chemical reactions do not affect overall gas and liquid flow, and (4) heat generation due to chemical reactions is neglected.

Two types of governing equations can be distinguished, multiphase flow and chemical transport. All flow and transport equations have the same structure, and can be derived from the principle of mass (or energy) conservation. Table 1 summarizes these equations and Table 2 gives the meaning of symbols used. The non-isothermal multi-phase flow consists of fluid flow in both liquid and gas phases, and heat transport, which has been discussed in detail by *Pruess* [1987 and 1991]. Aqueous (dissolved) species are subject to transport in the liquid phase as well as to local chemical interactions with the solid and gaseous phases. Transport equations are written in terms of total dissolved concentrations of chemical components which are concentrations of their basis species concentrations plus their associated aqueous secondary species [*Yeh and Tripathi*, 1991; *Steeffel and Lasaga*, 1994; *Walter et al.*, 1994; and *Lichtner*, 1996]. Advection and diffusion processes are considered for both the liquid and gas phases, and their coefficients are assumed to be the same for all species. The local chemical interactions in the transport equations are represented by the reaction source/sink terms. For transport in the liquid

phase, these source terms are q_{js} (in Table 1) representing mass transfer from the solid to the liquid phase, and q_{jg} from the gas to the liquid phase. For transport in the gas phase, the reaction source term is $-q_{jg}$ representing mass transfer from the liquid to the gas phase.

Table 1. Governing equations for fluid and heat flow, and chemical transport. Symbol meanings are given in Table 2.

| | | | |
|---|---|----------------------------------|--|
| General governing equations: | $\frac{\partial M_{\kappa}}{\partial t} = -\nabla F_{\kappa} + q_{\kappa}$ | | |
| Water: $M_w = \phi(S_l \rho_l X_{wl} + S_g \rho_g X_{wg})$ | $F_w = X_{wl} \rho_l \mathbf{u}_l + X_{wg} \rho_g \mathbf{u}_g$ | $q_w = q_{wl} + q_{wg}$ | |
| Air: $M_a = \phi(S_l \rho_l X_{al} + S_g \rho_g X_{ag})$ | $F_a = X_{al} \rho_l \mathbf{u}_l + X_{ag} \rho_g \mathbf{u}_g$ | $q_a = q_{al} + q_{ag}$ | |
| Heat: $M_h = \phi(S_l \rho_l U_l + S_g \rho_g U_g) + (1-\phi)\rho_s U_s$ | $F_h = \sum_{\beta=l,g} h_{\beta} \rho_{\beta} \mathbf{u}_{\beta} - \lambda \nabla T$ | q_h | |
| <p style="text-align: center;">where $\mathbf{u}_{\beta} = -k \frac{k_{r\beta}}{\mu_{\beta}} (\nabla P_{\beta} - \rho_{\beta} \mathbf{g}) \quad \beta = l, g \quad \text{(Darcy's Law)}$</p> | | | |
| Chemical components in the liquid phase ($j = 1, 2, \dots, N_l$): | | | |
| $M_j = \phi S_l C_{jl}$ | $F_j = \mathbf{u}_l C_{jl} - D_l \nabla C_{jl}$ | $q_j = q_{jl} + q_{js} + q_{jg}$ | |
| Chemical components in the gas phase ($k = 1, 2, \dots, N_g$): | | | |
| $M_k = \phi S_l C_{kl}$ | $F_k = \mathbf{u}_g C_{kg} - D_g \nabla C_{kg}$ | $q_k = -q_{jg}$ | |
| <p style="text-align: center;">where $C_{kg} = f_{kg} / RT \quad \text{(gas law)}$</p> | | | |

Table 2. Symbols used in Table 1.

| | | | |
|----------------|---|-------------|--|
| C | component concentration, mol l ⁻¹ | ρ | density, kg m ⁻³ |
| D | diffusion coefficient, m ² s ⁻¹ | μ | viscosity, kg m ⁻¹ s ⁻¹ |
| F | mass flux, kg m ⁻² s ⁻¹ (*) | λ | heat conductivity, W m ⁻¹ K ⁻¹ |
| f | gaseous species partial pressure, bar | | |
| k | permeability, m ² | | |
| k _r | relative permeability | Subscripts: | |
| g | gravitational acceleration, m s ⁻² | a | air |
| M | mass accumulation, kg m ⁻³ | g | gas phase |
| N | number of chemical components | h | heat |
| P | pressure, Pa | j | chemical component in liquid phase |
| q | source/sink | k | chemical component in gas phase |
| S | saturation | l | liquid phase |
| T | temperature, °C | s | solid phase |
| U | internal energy, J kg ⁻¹ | w | water |
| u | Darcy velocity, m s ⁻¹ | κ | governing equation index |
| X | mass fraction | β | phase index |
| φ | porosity | | |

(*) For chemical transport and reaction calculations, molar units are used.

The primary governing equations given in Table 1 must be complemented with constitutive local relationships that express all parameters as functions of thermophysical and chemical variables. These expressions for non-isothermal multiphase flow are given by *Pruess* [1987]. The expressions for reactive chemical transport are given in the following section. The primary governing equations are nonlinear due to these local relationships.

2.2. Chemical reaction equations

A chemical species is defined as any chemical entity distinguishable from the rest due to (1) its elemental composition, and (2) by the phase in which it is present. For instance, gaseous CO₂ is a different species from aqueous CO₂. Not all species are needed to fully describe the chemical system. The subset of species which is strictly necessary is made up

of what are known as basis or master or primary species, or components [*Parkhurst et al.* 1980; *Reed*, 1982; *Yeh and Tripathi*, 1991; *Wolery*, 1992; *Steeffel and Lasaga*, 1994; and *Lichtner*, 1996]. The remaining species are called secondary species consisting of aqueous, precipitated (mineral), gaseous, exchanged, and surface complexes. The secondary species can be represented as a linear combination of the set of the basis species (Table 3). Aqueous complexation, gas dissolution/exsolution, cation exchange, and surface complexation are assumed to proceed according to the local equilibrium. Mineral dissolution/precipitation can proceed either subject to local equilibrium or kinetic constraints. Three types of equations are required for solving the chemical reaction system: mass action equations for equilibrium, rate expressions for kinetics, and mass balances for the basis chemical species (Table 3).

Table 3. List of chemical reaction equations: mass action, rate expression and mass balance (illustrated by specific examples; in fact the model is valid for general geochemistry). Symbol meanings are given in Table 4.

General dissociation reactions

$$S_i^s = \sum_{j=1}^{N_C} v_{ij} S_j^p$$

(1) General mass action equations:

$$K_i a_{S_i^s} = \sum_j^{N_C} (a_{S_j^p})^{v_{ij}}$$

Aqueous dissociation: $\text{HCO}_3^- = \text{CO}_3^{2-} + \text{H}^+$

$$K_{\text{HCO}_3^-} \gamma_{\text{HCO}_3^-} c_{\text{HCO}_3^-} = \gamma_{\text{CO}_3^{2-}} c_{\text{CO}_3^{2-}} \gamma_{\text{H}^+} c_{\text{H}^+}$$

Mineral dissolution: $\text{CaCO}_3(\text{s}) = \text{CO}_3^{2-} + \text{Ca}^{2+}$

$$K_{\text{CaCO}_3(\text{s})} = \gamma_{\text{Ca}^{2+}} c_{\text{Ca}^{2+}} \gamma_{\text{CO}_3^{2-}} c_{\text{CO}_3^{2-}}$$

Gas dissolution: $\text{CO}_2(\text{g}) = \text{CO}_2(\text{aq})$

$$K_{\text{CO}_2(\text{g})} f_{\text{CO}_2(\text{g})} = \gamma_{\text{CO}_2(\text{aq})} c_{\text{CO}_2(\text{aq})}$$

(2) Rate expressions:

$$r_m = k_m A_m [1 - (Q_m / K_m)^{\theta}]^{\eta} \quad \text{negative for precipitation}$$

Calcite dissolution rate (first order):

$$r_{\text{CaCO}_3(\text{s})} = k_{\text{CaCO}_3(\text{s})} A \left(1 - \frac{Q_{\text{CaCO}_3(\text{s})}}{K_{\text{CaCO}_3(\text{s})}} \right)$$

$$Q_{\text{CaCO}_3(\text{s})} = \gamma_{\text{Ca}^{2+}} c_{\text{Ca}^{2+}} \gamma_{\text{CO}_3^{2-}} c_{\text{CO}_3^{2-}} = K_{\text{CaCO}_3(\text{s})} \quad \text{at equilibrium}$$

(3) Conservation of chemical component in a closed chemical system:

Carbonate component CO_3^{2-} :

$$T_{\text{CO}_3^{2-}} = C_{\text{CO}_3^{2-}} + c_{\text{CO}_2(\text{g})} + c_{\text{CaCO}_3(\text{s})}$$

$$\text{where } C_{\text{CO}_3^{2-}} = c_{\text{CO}_3^{2-}} + c_{\text{HCO}_3^-} + c_{\text{CO}_2(\text{aq})} \quad (\text{total dissolved, subject to transport})$$

Table 4. Symbols used in Table 3. Note that some symbols that have been used in Table 1 have different meanings here.

| | | | |
|-------|---|----------------------|---|
| A | specific reactive surface area, $\text{m}^2 \text{kg}^{-1}$ | T | total concentration of component, mol l^{-1} |
| a | thermodynamic activity | | |
| C | total dissolved concentration of component, mol l^{-1} | S^p | basis species |
| c | species concentration, mol l^{-1} | S^s | secondary species |
| f | partial pressure of gas species, bar | γ | thermodynamic activity coefficient |
| Q | ion activity product | v | Stoichiometric coefficient |
| K | Equilibrium constant | | |
| k | kinetic rate constant, $\text{mol m}^{-2} \text{s}^{-1}$ | Subscript: | |
| N_c | number of component (basis species) | i | secondary species index |
| r | net dissolution rate, $\text{mol l}^{-1} \text{s}^{-1}$ | j | basis species index |
| S | species chemical formula | m | mineral index |
| | | n, θ , η | experimental parameters |

To help understand the formulation for chemical reactions, we selected a simple illustrative example in Table 3; in fact, our model is valid for any geochemical system. All reactions in Table 3 are written in dissociation forms, which are useful for facilitating mathematical modeling. For the mass action equations of aqueous dissociation, the activity is equal to the product of the activity coefficient and molar concentration. Aqueous species activity coefficients are calculated from the extended Debye-Hückel equation [Helgeson and Kirkham, 1974]. Activities of a pure mineral phase and H_2O are assumed to be one. Gases are assumed ideal, therefore, fugacity coefficients are assumed equal to one, and fugacity is equal to partial pressure (in bar). The mass action equations for cation exchange and surface complexation (double layer model) and activities for the surface species are calculated as in *Appelo and Postma* [1993], and *Dzombak and Morel* [1990]. Only mineral dissolution and precipitation are allowed to proceed subject to kinetics. The rate expression used is taken from *Lasaga et al.* [1994]. Mass conservation in the closed chemical system is written in terms of basis species. The species distribution must be

governed by the total concentration of the component. The total concentration of the surface species is its surface size. For cation exchange, it is equal to cation exchange capacity (so called CEC).

Redox reactions are written in terms of aqueous oxygen such as, $\text{HS}^- = \text{SO}_4^{2-} - 2\text{O}_2(\text{aq}) + \text{H}^+$, or hypothetical electron, $\text{HS}^- = \text{SO}_4^{2-} - 4\text{H}_2\text{O} + 8\text{e}^- + 9\text{H}^+$. Using these two approaches, mathematical equations for redox reactions have the same form as other types of reactions [Liu and Narasimhan, 1989].

3. Model implementation

3.1. Solution method

The coupled model is implemented by introducing multi-component transport and reactive chemistry into the framework of the existing non-isothermal multi-phase flow computer code TOUGH2 [Pruess, 1991], resulting in the general reactive chemical transport code TOUGHREACT. Our model uses a sequential iteration approach [Cederberg et al., 1985; Yeh and Tripathi 1991, Simunek and Soares, 1994, Walter et al., 1994]. The flow and transport in geologic media is based on space discretization by means of integral finite differences [Narasimhan and Witherspoon, 1976]. An implicit time-weighting scheme is used for flow, transport, and geochemical reaction. Full details of the numerical solution for transport are given in [Xu et al., 1997]. An improved equilibrium-kinetics speciation model for simulating water-rock-gas interaction is employed [see Xu et al., 1998b]. In this reaction model, equilibrium and kinetics are solved simultaneously by Newton-Raphson iteration, which allows a larger time step to be applied. In addition, the

Newton-Raphson iteration scheme has been modified such that the unknowns are the relative concentration increments as opposed to their absolute values. By doing this, the modified Jacobian matrix is symmetric and better conditioned, improving convergence. Full details are given in *Xu et al.* [1998b].

The flow chart of the computer simulator TOUGHREACT is presented in Figure 1. The non-isothermal multiphase flow equations are solved first, and the resulting fluid velocities and phase saturations are used for transport simulation. Transport in the liquid phase is treated in terms of total dissolved concentrations. In addition, if gaseous species are present, the transport is solved in terms of their partial pressures. The resulting concentrations and partial pressures from the transport calculation are substituted into the chemical reaction model. The temperature distribution obtained from the solution of the multiphase flow equations is used to update physical and chemical parameters. The chemical transport equations are solved component by component, whereas the reaction equations are solved on a grid block basis. The transport and reaction equations are solved iteratively until convergence.

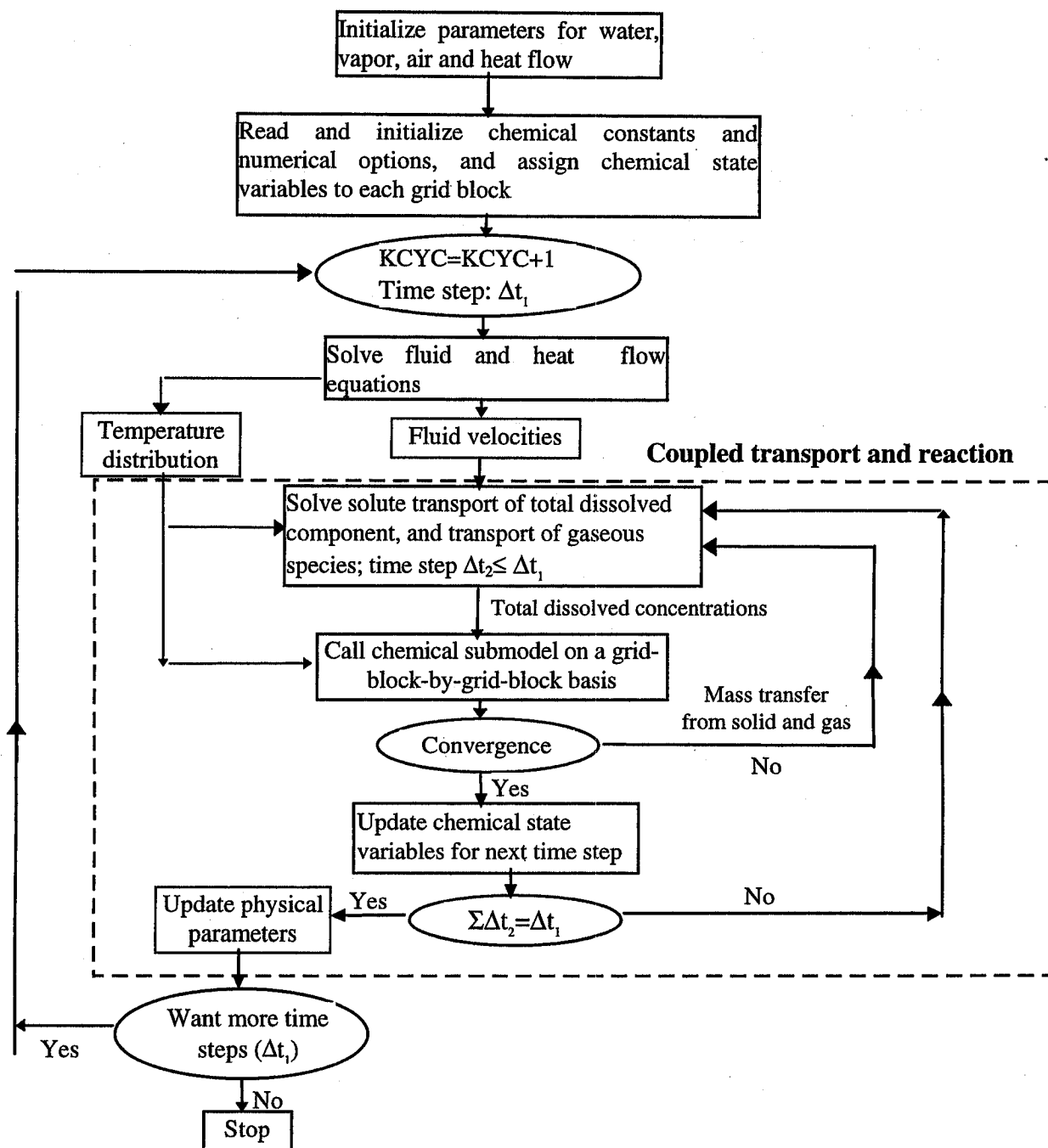


Figure 1. Flow chart of coupled model TOUGHREACT for non-isothermal multiphase flow, solute and reactive chemistry.

3.2. Quasi-stationary states

Reactive chemical transport may occur on a broad range of time scales. After a brief transient evolution, reactive systems may settle into a "quasi-stationary state" [QSS; *Lichtner*, 1988], during which aqueous concentrations of all chemical species remain essentially constant. Dissolution of primary and precipitation of secondary minerals proceed at constant rates. In fact, no complex calculations are necessary and only abundances of mineral phases need to be updated. This state terminates when one or more minerals dissolve completely at any of the grid blocks. A relative concentration change, δ_c , and a relative dissolution (or precipitation) rate change, δ_r , are used to monitor attainment of the QSS conditions,

$$\delta_c = \max_{\substack{\text{all components} \\ \text{all grid blocks}}} \left| \frac{C^{k+1} - C^k}{C^k} \right| < \epsilon_c \quad (1a)$$

$$\delta_r = \max_{\substack{\text{all minerals} \\ \text{all grid blocks}}} \left| \frac{r^{k+1} - r^k}{r^k} \right| < \epsilon_r \quad (1b)$$

where k is the transport time step index, C are dissolved component concentrations, r are dissolution or precipitation rates, and ϵ_c and ϵ_r are the QSS tolerances. This is of considerable practical importance, because substantially larger time steps should be possible during periods where a QSS is present [*Neretnieks*, 1997].

3.3. Time stepping

The solution of the nonlinear reactive transport equations involves several iterative procedures. Each iterative procedure is performed until convergence is achieved. Convergence is very sensitive to the initial estimates of concentrations. At a given time step, initial concentrations are taken equal to those computed at the previous time step. For the first time step, the estimates are taken from the initial concentrations which in some cases may be very different from the true solution. In some cases such as redox reactions a very small time increment may be required in order to give a close initial estimate. Time steps can be increased gradually up to a maximum value when approaching a QSS. An automatic time stepping scheme is implemented in TOUGHREACT. Three time step levels are used. The global time step, Δt_1 , is controlled by the solution of the flow equations. During a time interval of Δt_1 , depending on convergence, multiple steps Δt_2 , with $\sum \Delta t_2 = \Delta t_1$ can be used for solution of transport. Similarly, $\sum \Delta t_3 = \Delta t_2$ (where Δt_3 is the reaction time step) can be used for reaction calculations. The Δt_3 pattern may be different from grid block to grid block depending on the convergence behavior of the local chemical reaction system. For example, at the redox front a small Δt_3 may be required.

3.4. Model capabilities

The main features of the TOUGHREACT computer model are listed in Table 5. General multiphase flow and chemical transport conditions are considered. The model can take into account any number of species present in liquid, gas and solid phases. It is well

suited for reactive chemical transport in variably saturated porous and fractured media under non-isothermal multiphase flow conditions.

Table 5. Main features of the TOUGHREACT simulator for the coupled modeling of subsurface non-isothermal multiphase flow, solute transport and chemical reactions.

| Term | Feature |
|--|--|
| Dimensionality | 1-D, 2-D, or 3-D |
| Space discretization | Integral finite difference |
| Time integration | Implicit |
| Medium | Porous and fractured media; double porosity and dual permeability |
| Heterogeneity | Physical and chemical |
| Processes for non-isothermal multiphase flow | (1) Fluid flow in both liquid and gas phases occurs under pressure, viscous and gravity forces; (2) capillary pressure, vapor adsorption and vapor pressure lowering effects for the liquid phase; (3) heat flow by conduction, convection and diffusion |
| Processes for transport of aqueous and gaseous species | Advection and diffusion |
| Linear equation solver for flow and transport | MA28 (LU direct) or preconditioned conjugate gradient (iterative) |
| Equilibrium reactions | Aqueous complexation, acid-base, redox, mineral dissolution/precipitation, gas dissolution/exsolution, cation exchange, and surface complexation |
| Kinetics | Mineral dissolution/precipitation |
| Chemical data base | Modified EQ3/6 data base |

4. Verification and validation

Verification of non-isothermal multiphase flow is given by *Pruess* [1987, 1991] and *Pruess et al.* [1996]. Here we only present the verification of mineral dissolution against analytical solutions, and of pyrite oxidation in unsaturated-saturated flow conditions against TOUGH2-CHEM [White, 1995]. TOUGH2-CHEM computer program is also based on the framework of the non-isothermal multi-phase flow program TOUGH2, and employs a fully coupled approach where all flow and reactive transport equations are solved simultaneously. TOUGH2-CHEM was designed primarily for reactive flow and transport in geothermal reservoir systems. A simulation of water quality in the Aquia aquifer (Maryland) is presented to validate the model for a field scale problem. In addition, cation exchange and surface complexation were verified using other numerical simulators.

4.1. Mineral dissolution

We consider one-dimensional transport of two hypothetical species A and B, which originate from the dissolution of a mineral phase AB_s , $AB_s \Leftrightarrow A + B$, in a semi-infinite water saturated medium under a steady uniform velocity flow regime. This problem can be solved analytically for both equilibrium and kinetic conditions (see Appendix). Parameters used in the TOUGHREACT simulation are listed in Table 6. The numerical results for both conditions agree well with the analytical solutions (Figure 2).

Table 6. Parameters used for the TOUGHREACT verification of the mineral dissolution.

| Parameter | value |
|--|---------------------|
| Length (m) | 1.0 |
| Grid size (m) | 0.04 |
| Pore velocity (m day ⁻¹) | 0.1 |
| Porosity | 0.4 |
| Equilibrium constant | 10 ⁻⁸ |
| Kinetic rate constant (mol s ⁻¹ m ⁻²) | 2×10 ⁻¹⁰ |
| Specific surface area (m ² l ⁻¹) | 1.0 |
| Initial concentrations (mol l ⁻¹) | |
| Species A | 10 ⁻⁴ |
| Species B | 10 ⁻⁴ |
| Boundary concentrations (mol l ⁻¹) | |
| Species A | 10 ⁻⁵ |
| Species B | 10 ⁻⁴ |

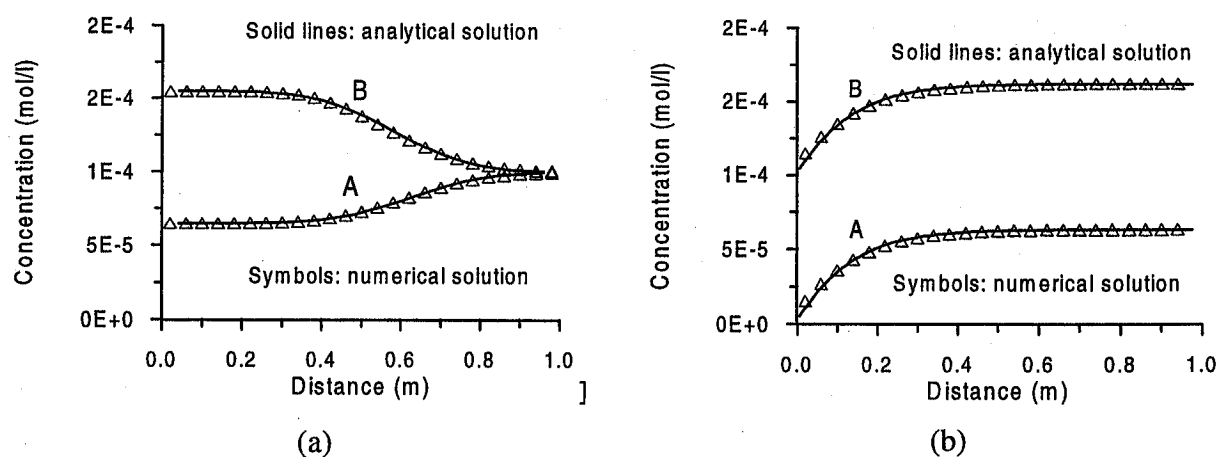


Figure 2. Concentration profiles for two species A and B in a problem involving dissolution of a mineral AB₅ under conditions of local equilibrium (a) and kinetic rates (b).

An additional run was performed for kinetic mineral dissolution with rate constant increased from $k = 2.0 \times 10^{-10}$ to $2.0 \times 10^{-8} \text{ mol s}^{-1} \text{ m}^{-2}$. Figure 3 shows that kinetic results are closer to equilibrium (Figure 2a) when the rate constant increases.

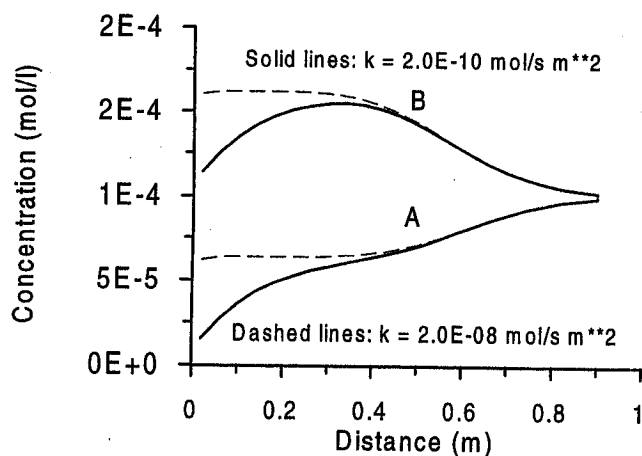


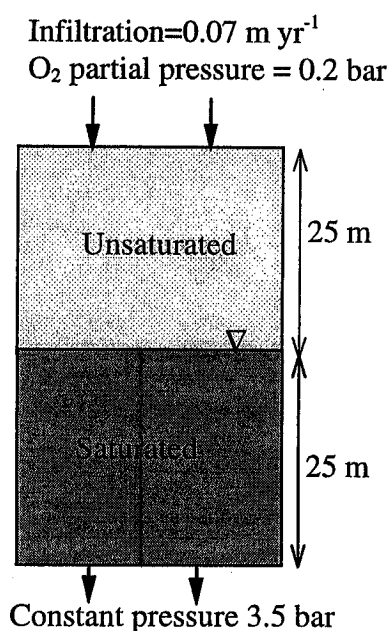
Figure 3. Simulated concentrations at 6 days for two different kinetic rate constants k .

4.2. Pyrite oxidation in a variably saturated medium

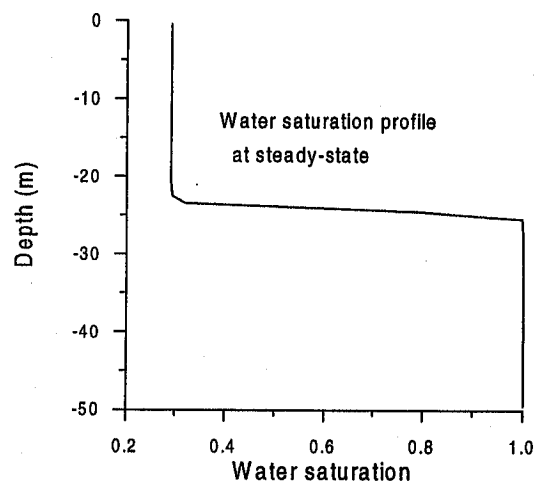
Pyrite (FeS_2) oxidation plays an important role in the genesis of enriched ore deposits through weathering reactions, and is the primary source of acid drainage from mines and waste rock piles. A prototype for oxidative weathering processes of pyrite in an unsaturated-saturated medium has been simulated with TOUGHREACT, and compared with TOUGH2-CHEM [White, 1995; Xu *et al.*, 1998c].

A vertical column is modeled, which extends from the atmosphere through an unsaturated zone, and below the water table (Figure 4a). Oxygen is supplied to the top of

the column as a dissolved species in infiltrating rainwaters and is also transported by gaseous diffusion from the land surface boundary. The initial flow conditions are set by specifying the rate of water infiltration into the top of the model (0.07 m yr^{-1}) and a constant pressure of 3.5 bar at the bottom. The steady-state water saturations (Figure 4b) obtained by ignoring chemical reactions are used as initial conditions for the calculation of reactive chemical transport. Parameters for this unsaturated-saturated medium are listed in Table 7.



(a)



(b)

Figure 4. (a) Schematic representation of the unsaturated-saturated flow system used for pyrite oxidation, and (b) the steady-state water saturation distribution.

Table 7. Physical parameters used for the unsaturated-saturated flow system.

| Parameter | Value |
|--|----------------------|
| Infiltration (m yr^{-1}) | 0.07 |
| Depth (m) | 50 |
| Grid spacing (m) | 1 |
| O_2 partial pressure at the land surface (bar) | 0.2 |
| Permeability (m^2) | 7×10^{-12} |
| gas O_2 diffusivity ($\text{m}^2 \text{s}^{-1}$) | 4.4×10^{-5} |
| Tortuosity | 0.1 |
| Porosity | 0.1 |
| Relative permeability and capillary pressure [van Genuchten, 1980]: | |
| λ | 0.457 |
| S_{lr} | 0.05 |
| S_{ls} | 1.0 |
| $P_0(\text{Pa})$ | 1.96×10^3 |

Reactions considered are listed in Table 8. Aqueous dissociation and gas dissolution are assumed to proceed according to the local equilibrium. Pyrite oxidation is subject to kinetic constraint. A kinetic rate constant of $2 \times 10^{-10} \text{ mol m}^{-2} \text{s}^{-1}$ and a specific surface area of $58.67 \text{ m}^2 \text{m}^{-3}$ are used. The initial water composition corresponds to a dilute reducing water with aqueous oxygen concentration, $c_{\text{O}_2(\text{aq})}$, of $1.0 \times 10^{-70} \text{ mol l}^{-1}$. The infiltration water composition corresponds to a dilute oxidizing water with $c_{\text{O}_2(\text{aq})} = 2.53 \times 10^{-4}$ which is at equilibrium with an atmospheric O_2 partial pressure of 0.2 bar. Initial pyrite abundance is 9% by volume.

Table 8. List of reactions involved in pyrite oxidation. Thermodynamic equilibrium constants are from the EQ3/6 database [Wolery, 1992].

| Reaction | $\log_{10}K$ at 25 °C |
|--|-----------------------|
| $O_2(g) = O_2(aq)$ | -2.898 |
| $\text{pyrite}(\text{FeS}_2) + 7/2 O_2(aq) + H_2O = 2H^+ + 2SO_4^{2-} + Fe^{2+}$ | 217.4 |
| $HS^- + 2O_2(aq) = H^+ + SO_4^{2-}$ | 138.32 |
| $H_2S(aq) + 2O_2(aq) = 2H^+ + SO_4^{2-}$ | 131.33 |
| $Fe^{2+} + 1/4 O_2(aq) + H^+ = Fe^{3+} + 1/2 H_2O$ | 8.475 |
| $OH^- + H^+ = H_2O$ | 13.995 |
| $HSO_4^- = H^+ + SO_4^{2-}$ | -1.9791 |
| $FeSO_4(aq) = SO_4^{2-} + Fe^{2+}$ | -2.2 |

The results for pH and total dissolved S are shown in Figure 5. The TOUGHREACT and TOUGH2-CHEM simulations agree well for the quasi-stationary states (QSS), but show some differences during the transient approach to the QSS, which is attributed to the somewhat different process descriptions. Full details are given in *Xu et al* [1998c].

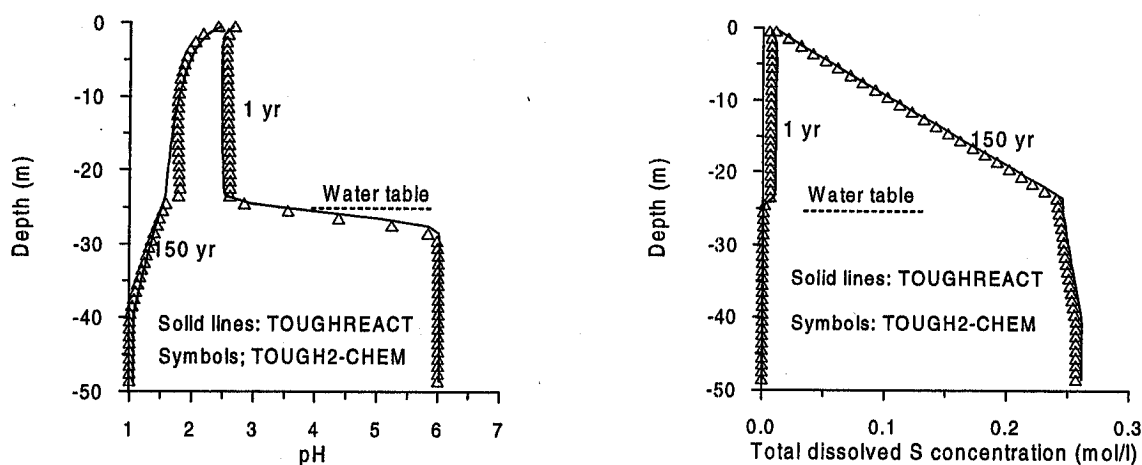


Figure 5. pH and total dissolved S as simulated with TOUGHREACT and TOUGH2-CHEM for pyrite oxidation in an unsaturated-saturated medium.

4.3. Water quality in the Aquia aquifer, Maryland

NaHCO_3 type waters in the coastal plain aquifers of the eastern United States have been related to freshening of the aquifer [Chapelle and Knobel, 1983]. These investigators depict major cation patterns as a function of flow length in the Aquia aquifer (Maryland). The water quality in this aquifer shows zonal bands with changes in concentrations of major cations that have been attributed to cation exchange and calcite dissolution/precipitation.

The observed water quality pattern was previously simulated with PHREEQM by Appelo [1994]. In the present TOUGHREACT simulation, hydrological conditions considered and all data used are the same as Appelo [1994]. The aim is to validate our model applicability to field scale problems. Figure 6 shows a schematic cross section along

a flow path. The aquifer is bounded to the east by a change in facies. The prepumping hydraulic head distribution suggests a confined aquifer in the upstream half and gradual loss of water in the downstream part of the aquifer [Chapelle and Drummond, 1983]. Leakage probably occurs via Pleistocene channels which cut through the confining beds. The hydrological conditions have been modeled assuming a one-dimensional flow tube with recharge at $x=0$, and with seepage into the confining layers evenly distributed over the second half of the flow tube.

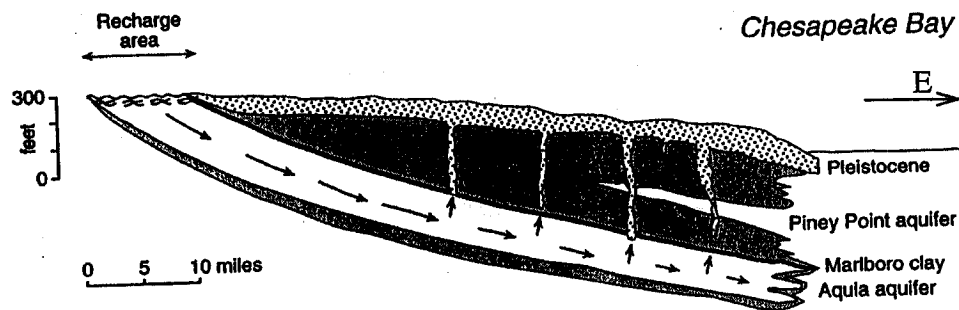


Figure 6. Schematic cross section of the Aquia aquifer (Maryland) adapted from Appelo [1994]. Recharge occurs in the outcrop of the formation: discharge is schematized to take place evenly in the downstream half. (1 foot equals 0.3048 m; 1 mile equals 1.609 km)

It was assumed that the initial water quality was brackish as a result of mixing of seawater with fresh water during deposition of the overlying Marlboro clay, which is a brackish water clay. The recharge water quality is presumed to be unchanged from that analyzed in the upstream reaches of the aquifer. The initial and recharge water compositions are presented in Table 9. These data are inferred from observations and

paleohydrochemical conditions. The detailed analysis and discussion are given by *Appelo* [1994]. To obtain recharge water quality in the first 10 miles (16 km) of the flow path, the exchange capacity for the first 10 miles was set to zero. The reactions considered in this simulation are listed in Table 10.

Table 9. Initial and recharge water composition (concentrations are given in mmol/l) for modeling the water quality patterns in the Aquia aquifer. X^- represents cation exchange sites. Data are from *Appelo* [1994]

| | pH | Na ⁺ | K ⁺ | Mg ²⁺ | Ca ²⁺ | Cl ⁻ | HCO ₃ ⁻ | SO ₄ ²⁻ | X ⁻ |
|----------|------|-----------------|----------------|------------------|------------------|-----------------|-------------------------------|-------------------------------|----------------|
| Initial | 6.80 | 87.4 | 1.9 | 9.92 | 4.38 | 101.8 | 15.5 | 0.27 | 200 |
| Recharge | 7.57 | 0.1 | 0.05 | 0.0 | 1.40 | 0.1 | 2.8 | 0.0 | |

Table 10. List of chemical reactions considered for modeling the water quality patterns in the Aqua aquifer. The cation selectivity used is based on Appelo [1994].

| Chemical reactions | $\log_{10}(K)$ at 25 °C |
|---|-------------------------|
| Aqueous dissociation: | |
| $\text{OH}^- = \text{H}_2\text{O} - \text{H}^+$ | 13.995 |
| $\text{CO}_3^{2-} = \text{HCO}_3^- - \text{H}^+$ | 10.329 |
| $\text{CO}_2(\text{aq}) = \text{HCO}_3^- + \text{H}^+ - \text{H}_2\text{O}$ | -6.3447 |
| $\text{CaHCO}_3^+ = \text{Ca}^{2+} + \text{HCO}_3^-$ | -1.0467 |
| $\text{MgHCO}_3^+ = \text{Mg}^{2+} + \text{HCO}_3^-$ | -1.0357 |
| $\text{CaCO}_3(\text{aq}) = \text{Ca}^{2+} + \text{HCO}_3^- - \text{H}^+$ | 7.0017 |
| $\text{MgCO}_3(\text{aq}) = \text{Mg}^{2+} + \text{HCO}_3^- - \text{H}^+$ | 7.3499 |
| $\text{NaHCO}_3(\text{aq}) = \text{Na}^+ + \text{HCO}_3^-$ | -0.1541 |
| $\text{CaSO}_4(\text{aq}) = \text{Ca}^{2+} + \text{SO}_4^{2-}$ | -2.1111 |
| $\text{MgSO}_4(\text{aq}) = \text{Mg}^{2+} + \text{SO}_4^{2-}$ | -2.309 |
| $\text{NaSO}_4^- = \text{Na}^+ + \text{SO}_4^{2-}$ | -0.82 |
| $\text{KSO}_4^- = \text{K}^+ + \text{SO}_4^{2-}$ | -0.8796 |
| Cation exchange: | |
| $\text{Na}^+ + 0.5\text{Ca-X}_2 = 0.5\text{Ca}^{2+} + \text{Na-X}$ | -0.4 |
| $\text{Na}^+ + 0.5\text{Mg-X}_2 = 0.5\text{Mg}^{2+} + \text{Na-X}$ | -0.3 |
| $\text{Na}^+ + \text{K-X} = \text{K}^+ + \text{Na-X}$ | -0.7 |
| $\text{Na}^+ + \text{H-X} = \text{H}^+ + \text{Na-X}$ | 5.883 |
| mineral dissolution | |
| $\text{Calcite} = \text{Ca}^{2+} + \text{HCO}_3^- - \text{H}^+$ | 1.8487 |

A pore velocity of 2.42 mile/ka was used in the upper part of the aquifer. A porosity of 0.3 was used throughout. Dispersivity was set to 2.0 miles (3.2 km) in the upper part, which is optimized by trial and error [Appelo 1994]. In the downstream zone where the confining beds are leaky, a zero dispersivity was assumed following the previous investigator.

The TOUGHREACT results are compared with observations for major cations and alkalinity (Figure 7). The present model results are practically identical to those obtained with PHREEQM [Appelo, 1994]. The agreement between numerical results and observations is reasonably satisfactory. The sequential appearance of Mg^{2+} and K^+ is attributed to chromatographic separation and can be varied in the model only by varying the $\text{Mg}^{2+}/\text{K}^+$ selectivity. An apparent dip in alkalinity is observed just before Na^+ concentrations increase, which is matched by the simulation. The upstream increase of Ca^{2+} concentrations in the region where K^+ and Mg^{2+} are peaking indicates an increased concentration of Ca-X_2 (X represents cation exchange sites). The increase occurred during flushing of Na^+ and is due to dissolution of calcite. The increase of Na^+ and alkalinity at the downstream end agree with earlier conclusions about the development of NaHCO_3 water quality in a freshening aquifer [Chapelle and Knobel, 1983].

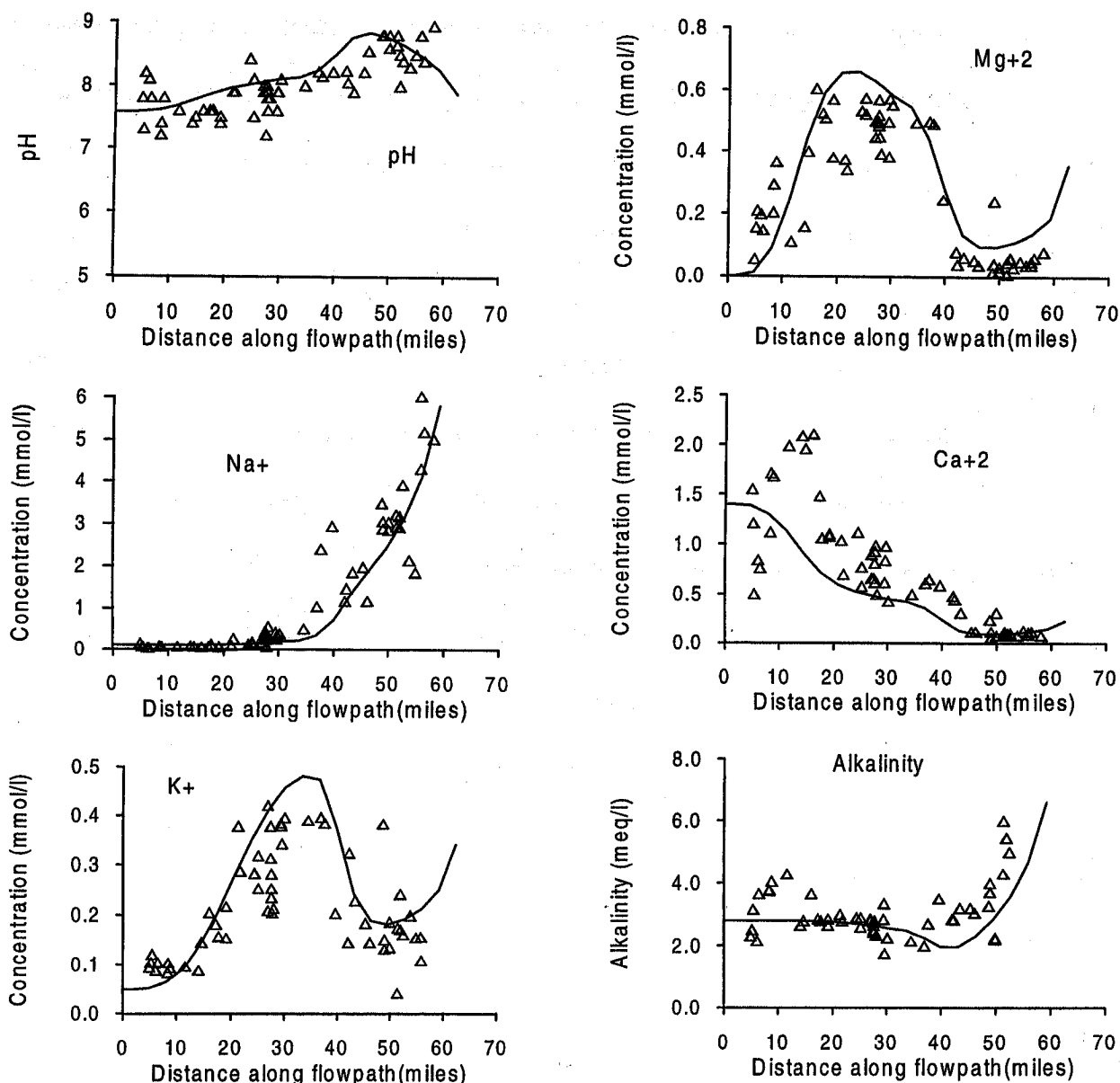


Figure 7. Concentrations of Na^+ , K^+ , Mg^{2+} , Ca^{2+} , alkalinity and pH along a flow path in the Aquia aquifer (Maryland). Symbols indicate observations that are provided by Appelo [1994] and originally from Chapelle and Knobel [1983]; solid lines represent simulated concentrations using TOUGHREACT.

5. Conclusions

A general coupled model, TOUGHREACT, for subsurface non-isothermal multiphase flow, solute transport and reactive chemistry has been developed. A wide range of thermo-physical-chemical processes is considered. The model can be applied to one-, two-, or three-dimensional porous and fractured media with physical and chemical heterogeneity. A variety of equilibrium chemical reactions are considered such as aqueous complexation, gas dissolution/exsolution, cation exchange, and surface complexation. Mineral dissolution/precipitation can proceed either subject to local equilibrium conditions or kinetics. The coupled model employs a sequential iteration approach. To improve the efficiency, monitoring for quasi-stationary states and automatic time stepping are implemented in the program. The model has been verified for a variety of physical and chemical processes. A simulation of water quality in the Aquia aquifer, Maryland, has been performed as model validation. The model is well suited for reactive chemical transport in variably saturated porous and fractured media under non-isothermal multiphase flow conditions. In the second of this two-part paper [this issue], three applications covering a range of reactive transport problems are presented to illustrate the model capabilities.

Appendix: Analytical solution for a two-species mineral dissolution problem

Local equilibrium

Consider one-dimensional transport of two hypothetical species A and B which originate from the dissolution of a mineral phase AB_s , $AB_s \rightleftharpoons A + B$, in a semi-infinite medium under a steady-state uniform velocity flow regime. The transport equations for dissolved species A and B are given by

$$D \frac{\partial^2 c_A}{\partial x^2} - v \frac{\partial c_A}{\partial x} + r_{AB} = \frac{\partial c_A}{\partial t} \quad (\text{A.1a})$$

$$D \frac{\partial^2 c_B}{\partial x^2} - v \frac{\partial c_B}{\partial x} + r_{AB} = \frac{\partial c_B}{\partial t} \quad (\text{A.1b})$$

where c_A and c_B are concentrations of dissolved species A and B, v is pore water velocity, D is dispersion coefficient, and r_{AB} is the mineral dissolution rate (negative for precipitation). By subtracting (A.1a) from (A.1b), we have

$$D \frac{\partial^2 (c_B - c_A)}{\partial x^2} - v \frac{\partial (c_B - c_A)}{\partial x} = \frac{\partial (c_B - c_A)}{\partial t} \quad (\text{A.2})$$

The concentration difference of species A and B,

$$c_B - c_A = \psi \quad (\text{A.3})$$

obeys a standard advection-dispersion equation and behaves like a conservative solute. The solution of (A.2) in terms of this pseudo-conservative species ψ is given by van Genuchten and Alves [1982], as

$$\begin{aligned} \psi(x, t) = \psi_0 \cdot & \left\{ \frac{1}{2} \operatorname{erfc} \left(\frac{x - vt}{2\sqrt{Dt}} \right) + \sqrt{\frac{v^2 t}{\pi D}} \exp \left(-\frac{(x - vt)^2}{4Dt} \right) \right. \\ & \left. - \frac{1}{2} \left(1 - \frac{vx}{D} + \frac{v^2 t}{D} \right) \exp \left(\frac{vx}{D} \right) \operatorname{erfc} \left(\frac{x - vt}{2\sqrt{Dt}} \right) \right\} \end{aligned} \quad (\text{A.4})$$

where $\psi_0 = c_B^0 - c_A^0$ (concentrations at $x=0$).

Suppose the dissolved species A and B are at chemical equilibrium with the mineral AB_s . If concentrations of A and B are very small, their activity coefficients are close to one. According to the Mass-Action Law, we have

$$c_A c_B = K_{AB} \quad (\text{A.5})$$

where K_{AB} is the equilibrium (or solubility) constant. By substituting (A.3) into (A.5), we obtain

$$c_A^2 + \psi c_A - K_{AB} = 0 \quad (\text{A.6})$$

The solution of (A.6) is

$$c_A = \frac{\sqrt{\psi^2 + 4K_{AB}} - \psi}{2} \quad (\text{A.7})$$

Kinetic condition

The conditions are similar to the previous equilibrium case except the mineral AB_s dissolution based on kinetics. According to *Lasaga et al* [1994], the first order kinetic dissolution rate, r_{AB} , takes the form

$$r_{AB} = k\sigma \left(1 - \frac{c_A c_B}{K_{AB}} \right) \quad (A.8)$$

where k is the rate constant, σ is the specific reactive surface area, and K_{AB} is the equilibrium constant. k and σ can be practically considered as one parameter, $k\sigma$, which is called here rate coefficient (in mol/l/s).

The transport equations for dissolved species A and B can be solved for steady flow and negligible dispersion ($D=0$). Under these assumptions, Equations (A.1a) and (A.1b) reduce to

$$-v \frac{dc_A}{dx} + r_{AB} = 0 \quad (A.9a)$$

$$-v \frac{dc_B}{dx} + r_{AB} = 0 \quad (A.9b)$$

Subtracting (A.9a) from (A.9b) it follows that

$$-v \frac{d(c_B - c_A)}{dx} = 0 \quad (A.10)$$

indicating that $\psi = c_B - c_A$ remains constant. Let ψ_0 be the value of $(c_B - c_A)$ at $x=0$.

Then, c_A can be expressed as $c_A = c_B - \psi_0$, and substituted into (A.8),

$$r_{AB} = k\sigma \left(1 - \frac{c_B(c_B - \psi_0)}{K_{AB}} \right) \quad (\text{A.11})$$

Substituting this expression into (A.9b), leads to

$$-v \frac{dc_B}{dx} + k\sigma \left(1 - \frac{c_B(c_B - \psi_0)}{K_{AB}} \right) = 0 \quad (\text{A.12})$$

The solution of this ordinary differential equation is (detailed derivation is given in Xu [1996])

$$c_B = \frac{\lambda_1 - \lambda_2 \beta_0 \exp\left(-\frac{x}{d_e}\right)}{1 - \beta_0 \exp\left(-\frac{x}{d_e}\right)} \quad (\text{A.13})$$

where

$$\beta_0 = \frac{c_B^0 - \lambda_1}{c_B^0 - \lambda_2} \quad (\text{A.14})$$

$$d_e = \frac{vK_{AB}}{k\sigma(\lambda_1 - \lambda_2)} \quad (\text{A.15})$$

λ_1 and λ_2 are the roots of the following second-order polynomial equation ($\lambda_1 \geq \lambda_2$)

$$\lambda^2 - \psi_0 \lambda - K_{AB} = 0 \quad (\text{A.16})$$

Acknowledgement.

The authors appreciate stimulating discussions with George Brimhall, John Apps, Eric Sonnenthal, Nicolas Spycher, Frederic Gérard, and Tom Wolery. We like to thank to Tony Appelo for providing validation data for the Aquia auifer. We are grateful to Nicolas Spycher and Curtis Oldenburg for a careful review of this manuscript and the suggestion of improvements. This work was supported by the Laboratory Directed Research and Development Program of the Ernest Orlando Lawrence Berkeley National Laboratory, under U.S. Department of Energy Contract No. DE-AC03-76SF00098.

References

- Ague, J. J., and G. H. Brimhall, Geochemical modeling of steady state and chemical reaction during supergene enrichment of porphyry copper deposits, *Econ. Geol.*, 84, 506-528, 1989.
- Appelo, C. A. J., and D. Postma, Geochemistry, groundwater and pollution, Free University, Amsterdam, The Netherlands, 1993.
- Appelo, C. A. J., Cation and proton exchange, pH variations and carbonate reactions in a freshening aquifer, *Water Resour. Res.*, 30(10), 2793-2805, 1994.
- Cederberg, G. A., R. Street, and J. O. Leckie, A groundwater mass transport and equilibrium chemistry model for multicomponent systems, *Water Resour. Res.*, 21(8), 1095-1104, 1985.
- Chapelle, F. H., and D. D. Drummond, Hydrogeology, digital simulation, and geochemistry of the Aquia and Piney Point-Nanjemoy aquifer system in southern Maryland, *Rep. Invest.* 38, Md. Geol. Surv., Baltimore, Maryland, 1983
- Chapelle, F. H., and L. L. Knobel, Aqueous geochemistry and exchangeable cation composition of glauconite in the Aquia aquifer, Maryland, *Ground water*, 21, 343-352, 1983
- Dzombak, D. A., and F. M. M. Morel, Surface complexation modeling, *Wiley Interscience*, New York, 1990.

- Engesgaard, P., and K. L. Kipp, A geochemical transport model for redox-controlled movement of mineral fronts in groundwater flow systems: A case of nitrate removal by oxidation of pyrite, *Water Resour. Res.*, 28(10), 2829-2843, 1992.
- Helgeson, H. C., and D. H. Kirkham, Theoretical prediction of the thermodynamic behaviour of aqueous electrolytes at high pressures and temperatures: II. Debye-Hückel parameters for activity coefficients and relative partial molal properties, *Am. J. Sci.*, 274, 1199-1261, 1974.
- Lasaga, A. C., J. M. Soler, J. Ganor, T. E. Burch, and K. L. Nagy, Chemical weathering rate laws and global geochemical cycles, *Geochim. Cosmochim. Acta*, 58, 2361-2386, 1994.
- Lichtner, P.C. The quasi-stationary state approximation to coupled mass transport and fluid-rock interaction in a porous medium, *Geochim. Cosmochim. Acta*, Vol. 52, pp. 143 - 165, 1988.
- Lichtner, P. C., Continuum formulation of multicomponent-multiphase reactive transport, in *Reactive transport in porous media*, Reviews in Mineralogy, Vol. 34, 1-79, Mineral. Soc. of Am., 1996.
- Liu, C. W., and T. N. Narasimhan, Redox-controlled multiple species reactive chemical transport, 1. Model development, *Water Resour. Res.*, 25, 869-882, 1989.
- Narasimhan, T. N., and P. A. Witherspoon. An integrated finite difference method for analyzing fluid flow in porous media, *Water Res. Res.*, 12 (1), 57-64, 1976.
- Nienhuis, P., , C.A.T. Appelo, and A. Willemsen, Program PHREEQM: Modified from PHREEQE for use in mixing cell flow tube, Free University, Amsterdam, The Netherlands, 1991.
- Neretnieks, I., J. W. Yu, and J. Liu, An efficient time scaling technique for coupled geochemical and transport models, *J. Contam. Hydrology*, 26, 269-277, 1997
- Parkhurst, D. L., D. C. Thorstenson, and L. N. Plummer, PHREEQE: A computer program for geochemical calculations, US Geol. Surv. Water Resour. Invest. 80-96, 174 pp., 1980.
- Pruess, K., TOUGH user's guide, Nuclear Regulatory Commission, report NUREG/CR-4645 (also Lawrence Berkeley Laboratory Report LBL-20700, Berkeley, California), 1987.

- Pruess, K., TOUGH2: A general numerical simulator for multiphase fluid and heat flow, Lawrence Berkeley Laboratory Report LBL-29400, Berkeley, California, 1991.
- Pruess, K., A. Simmons, Y. S. Wu, and G. Moridis, TOUGH2 software qualification, Lawrence Berkeley National Laboratory Report LBL-38383, Berkeley, California, February, 1996.
- Reed, M.H., Calculation of multicomponent chemical equilibria and reaction processes in systems involving minerals, gases and aqueous phase, *Geochimica et Cosmochimica Acta*, Vol. 46, pp. 513-528, 1982.
- Simunek, J., and D. L. Suares, Two-dimensional transport model for variably saturated porous media with major ion chemistry, *Water Resour. Res.*, 30(4), 1115-1133, 1994.
- Steefel, C. I., and A. C. Lasaga, A coupled model for transport of multiple chemical species and kinetic precipitation/dissolution reactions with applications to reactive flow in single phase hydrothermal system, *Am. J. Sci.*, 294, 529-592, 1994.
- Steefel, C. I., and K. T. B. MacQuarrie, Approaches to modeling of reactive transport in porous media, In: Reactive transport in porous media, Lichtner, P. C., C. I. Steefel, and E. H. Oelkers (eds.), Reviews in Mineralogy, Vol. 34, 83-129, Mine. Soc. Am., 1996.
- Sun, Y., J. N. Petersen, T. P. Clement, and B. S. Hooker, Effect of reaction kinetics on predicted concentration profiles during subsurface bioremediation, *J. of Contam. Hydrology*, 31, 395-372, 1998.
- Van Genuchten, M. T., A closed-form equation for predicting the hydraulic conductivity of unsaturated soils, *Soil Sci. Soc. Am. J.*, 44(5), 892-898, 1980.
- Van Genuchten, M. T., and W. J. Alves, 1982, Analytical solutions of the one-dimensional convective-dispersive solute transport equation, U. S. Department of Agriculture, Technical Bulletin No. 1661, 151 pp.
- Viswanathan, H. S., Modification of the finite element heat and mass transfer code (FEHM) to model multicomponent reactive transport, Los Alamos National Laboratory Report LA-13167-T, 105 pp., Los Alamos, New Mexico, 1996.

- Walter, A. L., E. O. Frind, D. W. Blowes, C. J. Ptacek, and J. W. Molson, Modeling of multicomponent reactive transport in groundwater, 1, Model development and evaluation, *Water Resour. Res.*, 30 (11), 3137-3148, 1994.
- White, S. P., Multiphase non-isothermal transport of systems of reacting chemicals, *Water Resour. Res.*, 31 (7), 1761-1772, 1995.
- Wolery, T. J., EQ3/6, A software package for geochemical modeling of aqueous systems: Package overview and installation guide (version 7.0), Lawrence Livermore National Laboratory Report UCRL-MA-110662 PT I, Livermore, California, 1992.
- Xu, T., Modeling non-isothermal multicomponent reactive solute transport through variably saturated porous media, Ph.D. Dissertation, University of La Corunia, Spain, 1996.
- Xu, T., F. Gérard, K. Pruess and G. Brimhall, Modeling non-isothermal multiphase multi-species reactive chemical transport in geologic media, Lawrence Berkeley Laboratory Report LBL-40504, Berkeley, California, 1997.
- Xu, T., J. Samper and C. Ayora, Modeling of non-isothermal multi-species reactive transport in field-scale variably saturated media, *J. Hydrology*, In press, 1998a.
- Xu, T., K. Pruess and G. Brimhall. An improved equilibrium-kinetics speciation algorithm for redox reaction in variably saturated flow system, Submitted to *Computers & Geosciences* (also Lawrence Berkeley National Laboratory Report LBNL-41789, Berkeley, California), 1998b.
- Xu, T., S.P. White, and K. Pruess, Pyrite oxidation in saturated and unsaturated porous media flow: A comparison of alternative mathematical modeling approaches, Submitted to *Transport in porous media* (also Lawrence Berkeley National Laboratory Report LBNL-42049, Berkeley, California), 1998c.
- Yeh, G. T., and V. S. Tripathi, A critical evaluation of recent developments of hydrogeochemical transport models of reactive multichemical components, *Water Resour. Res.* 25(1), 93-108, 1989.
- Yeh, G. T., and V. S. Tripathi, A model for simulating transport of reactive multispecies components: model development and demonstration, *Water Resour. Res.* 27(12), 3075-3094, 1991.

Zysset, A., F. Stauffer and T. Dracos, Modeling of chemically reactive groundwater transport, *Water Resour. Res.*, 30 (7), 2217-2228, 1994.